Real-time imaging elucidates the role of H_2O_2 in regulating kinetics of epidermal growth factor-induced and Src-mediated tyrosine phosphorylation signaling

Ting Su
Xiangyong Li
Nisha Liu
Shaotao Pan
Jinling Lu
Jie Yang
Zhihong Zhang

Real-time imaging elucidates the role of H₂O₂ in regulating kinetics of epidermal growth factor-induced and Src-mediated tyrosine phosphorylation signaling

Ting Su,[a,b][*] Xiangyong Li,[a,b][*] Nisha Liu,[a,b] Shaotao Pan,[a,b] Jinling Lu,[a,b] Jie Yang,[a,b] and Zhihong Zhang[a,b]

[a]Britton Chance Center for Biomedical Photonics, Wuhan National Laboratory for Optoelectronics-Huazhong University of Science and Technology, Wuhan 430074, China

[b]MoE Key Laboratory for Biomedical Photonics, Department of Biomedical Engineering, Huazhong University of Science and Technology, Wuhan 430074, China

Abstract. Reversible oxidation is emerging as an important regulatory mechanism in protein tyrosine phosphorylation. Generation of hydrogen peroxide (H₂O₂), upon growth factor stimulation, is hypothesized to inhibit activity of protein tyrosine phosphatases (PTPs). This ensures that protein tyrosine kinases can elevate the steady-state level of protein tyrosine phosphorylation, which then allows propagation of the tyrosine phosphorylation signal. However, the effects of H₂O₂ on the kinetics of tyrosine phosphorylation signaling remain poorly understood, especially in living cells. Therefore, we used a genetically encoded Src kinase-specific biosensor based on fluorescence resonance energy transfer (FRET) to image the kinetics of the Src-mediated tyrosine phosphorylation signaling (Src signaling) induced by epidermal growth factor (EGF). We examined the kinetics under increased and decreased H₂O₂ levels. Through a straightforward, quantitative analysis method which characterized the signaling kinetics, we demonstrated that H₂O₂ modulated the amplitude and duration of the signal by inhibiting PTPs' activity. Our evidence also suggested the effect of H₂O₂ on Src activation is mediated by H₂O₂-dependent inhibition of PTPs. Furthermore, we provide evidence showing global elevation of intracellular H₂O₂ level attenuates EGF-induced Src signaling. © *2012 Society of Photo-Optical Instrumentation Engineers (SPIE).* [DOI: 10.1117/1.JBO.17.7.076015]

1 Introduction

Reversible protein tyrosine phosphorylation controls a wide range of fundamental cellular processes, including cell growth, adhesion, and proliferation. Because protein tyrosine kinases (PTKs) are counteracted by protein tyrosine phosphatases (PTPs), the tyrosine phosphorylation level of a given protein is the result of the concerted action of the related PTKs and PTPs.[1]

Recently, accumulating evidence reveals a critical role of H₂O₂-dependent modification in regulating tyrosine phosphorylation signaling that is induced by growth factors such as the epidermal growth factor (EGF)[2,3] and platelet-derived growth factor (PDGF).[4,5] H₂O₂ potentially inhibits activity of PTPs through oxidizing a cysteine in the active site of PTPs to create a cysteine-sulfenic derivative.[5–7] The current paradigm proposes that activation of PTKs is insufficient for elevating the steady-state level of protein tyrosine phosphorylation, and H₂O₂-mediated inhibition of PTPs is also required.[5] However, this proposal lacks real-time dynamic evidence in living cells.

Mathematical modeling has been applied to study control mechanisms of tyrosine phosphorylation signaling.[8,9] Two typical features of signaling, amplitude, and duration, have often been employed to characterize phosphorylation signaling. These two features possess biological consequences.[10] For example, in PC12 cells, sustained activation of extracellular signal-regulated protein kinase (ERK) by nerve growth factor (NGF) causes neuronal differentiation, whereas transient activation of ERK by EGF causes cell proliferation.[11] Previous work demonstrated that PTKs control the amplitude of tyrosine phosphorylation signaling, whereas PTPs mainly determine the duration of signaling.[8] However, these models were experimentally validated via western blotting, which requires damaging cells or tissue samples, and results in poor spatiotemporal resolution. The introduction of green fluorescence protein (GFP) into biology provides researchers with a noninvasive method to visualize protein behavior.[12] Additionally, combining GFP with fluorescence resonance energy transfer (FRET) technology gives birth to a variety of fluorescent biosensors capable of imaging and quantifying protein activities and cellular signals in living cells.[13–17] Thus, FRET-based biosensors are an ideal tool for illustrating the kinetics of tyrosine phosphorylation signaling in living cells.

The non-receptor cytoplasmic tyrosine kinase (cPTK) Src kinase was the first proto-oncogene to be discovered in the vertebrate genome.[18] Abundant evidence demonstrates the overexpression and abnormal activation of Src kinase are linked to the development of cancer.[19] Following growth factor treatment, cytoplasmic Src kinase is activated, which leads to phosphorylation of the specific tyrosine residues of downstream proteins, including focal adhesion proteins, adaptor proteins, and transcription factors. Src kinase is subject to diverse regulation,

including phosphorylation/de-phosphorylation, protein-protein interactions, and spatial localization.[19] Additionally, it was recently proposed that Src activity is regulated by redox modification via H_2O_2-mediated oxidation at cysteine residues.[20] However, the consequences of H_2O_2 dependent modification of Src kinase are still controversial. Both activation[21–23] and inactivation[24,25] of Src kinase by H_2O_2 have been reported. Conclusions regarding the effect of H_2O_2 on Src kinase came from studies based on *in vitro* purified Src protein and cell-based approaches involving western blotting. Therefore, it is necessary to evaluate the outcome of H_2O_2-dependent oxidation of Src kinase in living cells.

In this study, a genetically encoded Src kinase-specific biosensor (Src biosensor) based on FRET[26,27] was used to image the kinetics of EGF-induced Src signaling under increasing or decreasing hydrogen peroxide (H_2O_2) levels. The Src biosensor is encoded by a specific gene sequence, consisting of enhanced cyan fluorescent proteins (ECFP), the Src homology 2 (SH2 domain), a Src substrate peptide and Ypet, a yellow fluorescent protein (YFP) variant. Phosphorylation of the Src biosensor by Src kinase causes spatial separation of ECFP and Ypet, which leads to reduced energy transfer efficiency and the resulting increases in the cyan/yellow fluorescent protein (CFP/YFP) emission ratio. De-phosphorylation of the Src biosensor by PTPs results in a reduced CFP/YFP emission ratio. Because the tyrosine phosphorylation level of the Src biosensor is determined by the relative activity of Src kinase and PTPs, the CFP/YFP emission ratio of Src biosensor can be used to probe the kinetics of EGF-induced and Src-mediated tyrosine phosphorylation signaling (Src signaling). Any factors or processes influencing the kinetics of the CFP/YFP emission ratio of Src biosensor must be mediated by their effect on modulating activity of Src kinase or PTPs. To quantitatively characterize the effect of H_2O_2 on the kinetics of EGF-induced Src signaling in living cells, we introduced three parameters to extract the biological meanings of the CFP/YFP emission ratio of the Src biosensor. Through quantitatively analyzing those three parameters, we demonstrated that H_2O_2 modulates both the amplitude and the duration of EGF-induced Src signaling by inhibiting PTPs' activity.

2 Materials and Methods

2.1 Reagent

Human recombinant epithelial growth factor (EGF) was purchased from Peprotech (Rocky Hill, NJ). 5(6)-Carboxy-2',7'-dichlorofluorescein diacetate (carboxy-H2DCFDA), 4-Amino-5-(4-methylphenyl)-7-(t-butyl)pyrazolo[3,4-d]-pyrimidine (PP1), and sodium orthovanadate were purchased from Sigma-Aldrich (St. Louis, Missouri). Dulbecco's modified Eagle's medium (DMEM), Lipofectamine 2000 and CO_2-independent medium were purchased from Invitrogen (Carlsbad, CA). Restriction enzymes were purchased from New England Biolabs (Ipswich, Massachusetts). Vanadate was prepared from sodium orthovanadate according to previously reported method.[28]

2.2 Cell Culture and Transfection

HeLa cells were cultured in Dulbecco's modified Eagle's medium (DMEM) supplemented with 10% FBS, 100-U/ml penicillin, and 100-mg/ml streptomycin at 37°C in 5% CO_2.

Plasmids were transfected into HeLa cells by Lipofectamine 2000 according to manufacturer's instructions (Invitrogen).

2.3 Plasmid Construction

Ypet was generated by introducing S208F, V224L, H231E, and D234N into Venus. The architecture of our Src biosensor is identical to the previously reported Src biosensor.[26,27] Rac1 and Prx1 genes were amplified by PCR using cDNA prepared from HeLa cells. To generate the far-red fluorescent protein mLumin[29] tagged Rac1 (mLumin-Rac1), the mLumin fragment was amplified by PCR using a sense primer bearing a BamHI site and a reverse primer bearing an XhoI site. The Rac1 fragment was amplified by PCR using a sense primer bearing an XhoI site and a reverse primer bearing an EcoRI site. Finally, mLumin and Rac1 were ligated into pCDNA3.1 between BamHI and EcoRI sites. The PCR megaprimer method was used to generate mLumin-Rac1-N17.[30] For PrxI-Y194F, because Y194F is near the C-terminus, PrxI-Y194F was directly generated by normal PCR with an anti-sense primer bearing Y194F. To unambiguously identify cells expressing PrxI-Y194F, we used an internal ribosome entry site (IRES) sequence, which allowed expression of two genes from the same bi-cistronic mRNA transcript. The architecture of this sequence is as follows: BamHI-PrxI-(Y194F)-EcoRI-IRES-SacI-mLumin-NLS-XbaI. NLS represents nuclear localized sequence. First, IRES was amplified by PCR from a template pIRES vector (Invitrogen) with a sense primer bearing BamHI and EcoRI sites and an anti-sense primer bearing a SacI site. mLumin-NLS was obtained by PCR-addition of an NLS sequence (amino acid is PKKKRKVEDA) at the C-terminus of mLumin. This fragment was generated with SacI and XbaI sites at N- and C- terminus, respectively. Then, IRES and mLumin-NLS were fused into pCDNA 3.1 between the BamHI and XbaI sites. Finally, PrxI-Y194F was inserted before the IRES using BamHI and EcoRI restriction enzyme sites.

The mVenus gene is from Dr. Atsushi Miyawaki at Brain Science Institute, RIKEN, Japan.

2.4 Cell Imaging

Living cell imaging was performed on an Olympus confocal laser-scanning microscope FV1000 (Olympus, Japan) equipped with a 60×1.35 oil immersion objective. The FV1000 allows for dual-channel imaging. Thirty-six hours after transfection of exogenous plasmid, HeLa cells were starved for additional 6 to 12 h in serum-free DMEM before EGF (100 ng/ml) stimulation. Immediately before imaging, DMEM was replaced with CO_2-independent medium (Invitrogen). For the Src sensor, the following setting was used: 458-nm excitation, CFP emission: 470–500 nm, YFP emission: 520–560 nm. For mLumin, the 543-nm laser was used and emission wavelengths between 600 and 700 nm were collected. For the Grx1-roGFP2 biosensor, the following setting was used: 405- and 488-nm excitation, emission: 500–600 nm. The "time-control" function in the FV1000 software was used to quickly switch laser lines between 405 and 488 nm.

2.5 Image Processing

ImageJ software (http://rsbweb.nih.gov/ij/) was used to process confocal images and to generate the CFP/YFP emission ratio images of Src biosensor and the 405/488 nm excitation ratio images of Grx1-roGFP2 biosensor. The key procedures are identical with previous reports.[31,32] For Src biosensor, raw CFP and YFP images were firstly background subtracted at

each time point. Gaussian blur function (sigma value 1) was used for image smoothing. For each time point, because the YFP image had the largest signal-to-noise ratio, the YFP image was used to generate a binary mask image with a value of zero outside the cell and a value of one inside the cell. The CFP and YFP images were then respectively multiplied by this mask image. Finally, the updated CFP image was divided by the updated YFP image to yield the CFP/YFP emission ratio image of Src biosensor. For better visualization of ratiometric images, brightness/contrast was adjusted and a linear pseudo-color lookup table (color bar) was applied. For generating the kinetics of the normalized CFP/YFP emission ratio of Src biosensor, a region of interest in the cytoplasm of ratio images was selected to extract ratio values. And, the ratio values were normalized to the average ratio value before EGF stimulation by Excel (Microsoft).

For generating the $405/488$-nm excitation ratio images of Grx1-roGFP2, the image excited at 488 nm at each time point was used to generate a binary mask image. Then the following processing steps were identical with above procedures for generating the CFP/YFP ratio images of Src biosensor. For generating the kinetics of the normalized $405/488$-nm excitation ratio of Grx1-roGFP2, a region of interest in the cytoplasm of ratio images was selected to yield ratio values. Then the ratio values were normalized to the average ratio value before EGF or H_2O_2 stimulation by Excel (Microsoft).

The curves of the normalized CFP/YFP emission ratio of Src biosensor were plotted using OriginPro 8 software (Northampton, MA). The mathematical parameters, PAS and DS, were obtained from the curves of the normalized CFP/YFP emission

ratio of Src biosensor. And the ISS was calculated using integration function in OriginPro 8 software.

2.6 Statistical Analysis

The student's t-test function in GraphPad Prism software (San Diego, CA) was used to evaluate statistical differences between experimental groups. P values below 0.05 were considered as significantly different.

3 Results

3.1 Three Parameters to Quantitatively Characterize the Kinetics of Src Signaling upon EGF Stimulation

The CFP/YFP emission ratio of the Src biosensor provides an assay for measuring the magnitude and kinetics of Src signaling in living cells. To obtain the kinetics of Src signaling under EGF stimulation, HeLa cells were transfected with a plasmid encoding the Src biosensor. The concentration of EGF used throughout this study was 100 ng/ml. As shown in Fig. 1(a), activated Src mainly exists in the cytoplasm throughout the imaging period. Thus, a region of interest in the cytoplasm was selected for analyzing the kinetics of Src signaling. The kinetic profile of Src signaling upon EGF stimulation displayed biphasic characteristics, consisting of a rapidly increasing phase and a slowly declining phase [black curve in Fig. 1(b)]. Strikingly, the kinetic profile of EGF-induced Src signaling resembles kinetic profile of EGF-induced ERK-mediated phosphorylation signaling as reported before.[8–11] This similarity suggests that growth factor-induced
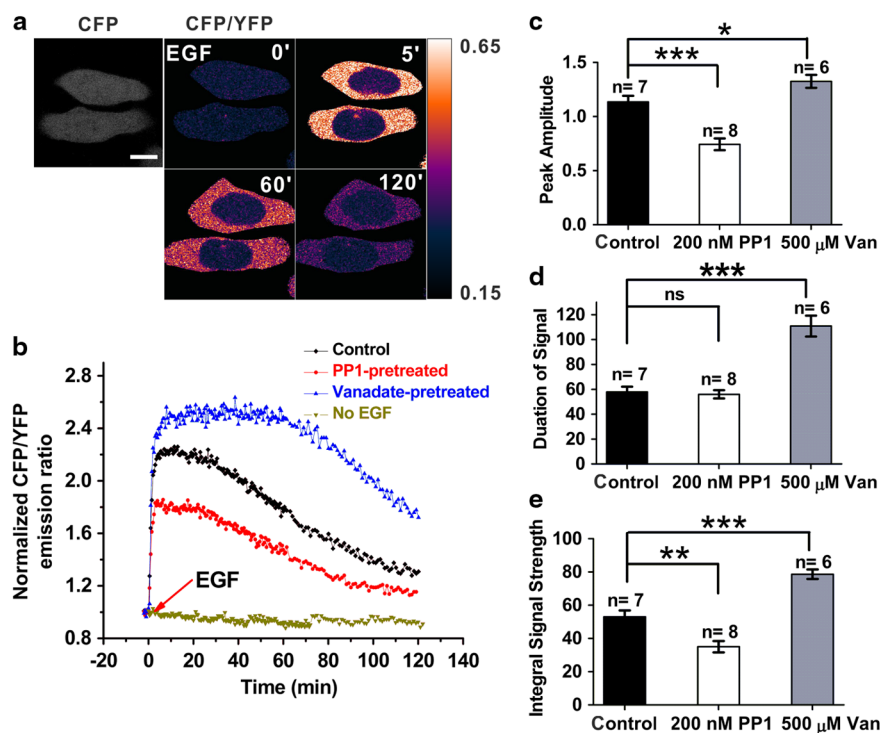

Fig. 1 Visualization of kinetics of epidermal growth factor (EGF)-induced Src signaling by Src biosensor; (a) Cyan/yellow fluorescent protein (CFP/YFP) emission ratio images of the Src biosensor in response to 100-ng/mL EGF; (b) Kinetics of normalized CFP/YFP emission ratios of the Src biosensor in response to EGF in a control HeLa cell as demonstrated in (a), or in a HeLa cell pre-treated with 200-nM PP1 (Src specific inhibitor) for 1 h, or in a HeLa cell pre-treated with 500-μM vanadate (PTP specific inhibitor, denoted as Van) for 30 min (c, d, and e). Bar graphs represent the mean $\pm$ SEM of peak amplitude, (c) duration, (d) and integral signal strength, (e) of Src signaling from at least three independent experiments with the same conditions, as in (b). "n" denotes the sample number in each group. "*", "**" and "***" indicate $p < 0.05$, $p < 0.01$ and $p < 0.001$ respectively. "ns" indicates insignificant differences between groups ($p > 0.05$). Scale bars, 10 μm.

and kinase-mediated phosphorylation signaling possesses analogous dynamic mechanisms. Therefore, we reasoned that the models concerning ERK signaling might be used to characterize EGF-induced Src signaling.[8,9,11] Based on previous models which described ERK phosphorylation signaling cascades,[8,9] we introduced the following three simplified mathematical parameters to more precisely define the kinetics of EGF-induced Src signaling: the peak amplitude of signaling (PAS), the duration of signaling (DS), and integral signaling strength (ISS). These parameters are calculated from the normalized CFP/YFP emission ratio curves (refer to Sec. 2.5 *Image Processing*), in which PAS is the maximum value of the normalized CFP/YFP emission ratio change within 5 min, DS is the full width of the curve at half of the maximum, and ISS is the area under the curve within 60 min.

To correlate the three kinetic parameters with the activity of Src kinase and PTP in living cells upon EGF treatment, PP1 and vanadate, which are specific inhibitors of Src kinase and PTPs, respectively, were used. As demonstrated in Fig. 1(a) and 1(b), exposure of HeLa cells to EGF led to rapid phosphorylation of the Src biosensor, and this phosphorylation was maintained at relatively high levels throughout the imaging session, demonstrating sustained activation of Src signaling [Fig. 1(c)–1(e); PAS: 1.14 ± 0.06; DS: 57.9 ± 4.2 min; ISS: 53.1 ± 3.8, $n = 7$]. The initially increasing phase typically reached a maximum value within 5 min, consistent with the experimentally tested model asserting that kinases are rapidly activated whereas phosphatases are transiently inhibited upon growth factor treatment, permitting rapidly signal amplification.[8,9] Hence, we conceived that Src activity is dominant to PTP activity in this phase. And PAS was used to measure the relative level of activated Src. We used this experiment as control group. Figure 1(b) demonstrates that inhibition of Src activity by PP1 resulted in marked decrease of PAS [Fig. 1(c); PAS: 0.74 ± 0.05, $n = 8$], whereas DS was not significantly influenced [Fig. 1(d); DS: 56.0 ± 3.3 min, $n = 8$]. Correspondingly, ISS was reduced due to decreases in the CFP/YFP ratio amplitude [Fig. 1(e); ISS: 35.0 ± 3.4, $n = 8$]. In contrast to effect of PP1, suppression of PTPs activity by vanadate led to a broader peak and substantially longer duration of CFP/YFP emission ratio [Fig. 1(b) and 1(d); DS: 110.8 ± 8.4 min, $n = 6$]. Additionally, there was a modest increase in PAS [Fig. 1(c); PAS: 1.33 ± 0.06, $n = 6$]. ISS was correspondingly increased with vanadate treatment [Fig. 1(e); ISS: 78.7 ± 2.8, $n = 6$].

Actually, vanadate alone is able to gradually induce weak activation of Src signaling (weakly activated pattern) [Fig. 2(b)],

but with quite different kinetics as compared to that of EGF-induced Src signaling (strongly activated pattern), suggesting those two stimulants utilize distinct mechanisms to initiate Src signaling. In some vanadate-pretreated HeLa cells upon EGF stimulation, those two types of kinetics co-exist and can be easily distinguished. As shown in Fig. 2(a), there is a slowly increasing phase after the rapidly increasing phase. Under this experimental condition, PAS values refer to the maximum value of the CFP/YFP emission ratio change within first 5 min following EGF treatment.

Taken together, when EGF induces Src signaling, Src kinase controls PAS [Fig. 1(c)], whereas PTPs have more effect on DS than PAS [Fig. 1(c) and 1(d)]. And, ISS is controlled by both Src kinase and PTPs [Fig. 1(e)]. Since the CFP/YFP emission ratio of Src biosensor is only determined by Src kinase and PTPs, the three kinetic parameters can be used to quantitatively assess how cellular regulators exert their effect on kinetics of Src signaling.

3.2 H_2O_2 Tunes the Duration of EGF-Induced Src Signaling Through PTP Inhibition

To investigate how H_2O_2 modulates the kinetics of Src signaling upon EGF stimulation, HeLa cells were transfected with two plasmids encoding two H_2O_2 regulating proteins: Rac1-N17 (dominant negative form of Rac1) and PrxI-Y194F (a variant of the H_2O_2 degrading enzyme PrxI).

A dominant negative form of Rac1 (Rac1-N17) is reported to prevent production of H_2O_2 through its inhibition of NADPH oxidase upon growth factor stimulation.[33–36] Actually, measurement of H_2O_2 by DCF dye showed that Rac1-N17 dramatically decreased intracellular EGF-induced H_2O_2 level (Fig. 3). To elucidate the role of H_2O_2 in regulating Src signaling, HeLa cells were co-transfected with two plasmids, encoding the Src biosensor and the far-red fluorescent protein mLumin[29] tagged Rac1-N17. We found that overexpression of Rac1-N17 remarkably prevented propagation of EGF-induced Src signaling [Fig. 4(a), 4(c), and 4(i); ISS: 26.4 ± 2.1, $n = 9$] and had more effects on DS than PAS [Fig. 4(g) and 4(h)]. In these cells, PAS was reduced to 0.92 ± 0.05 ($n = 9$; 19% lower than control) and DS was shortened to 23.2 ± 2.2 min ($n = 9$; 60% shorter than control). This result suggested that H_2O_2 production is critical to propagation of EGF-induced Src signaling.

To provide additional evidence, we decreased the amount of endogenous H_2O_2 by expressing a variant of the H_2O_2 degrading enzyme PrxI (Prx1-Y194F), which is an abundant cytosolic
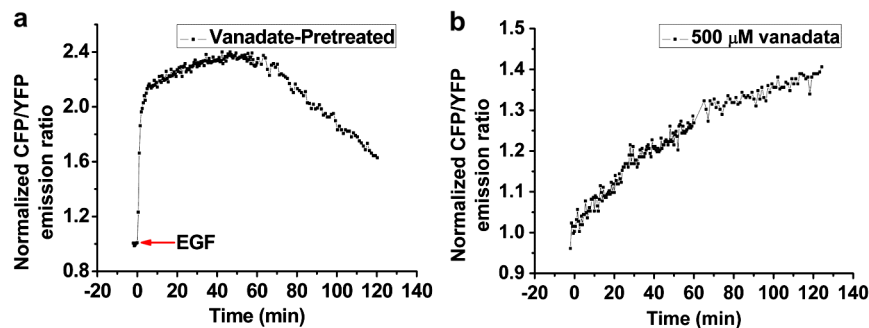

Fig. 2 Kinetics of normalized cyan/yellow fluorescent protein (CFP/YFP) emission ratios of the Src biosensor in response to EGF in a vanadate-pretreated HeLa cell; (a) Kinetics of normalized CFP/YFP emission ratios of the Src biosensor in response to epidermal growth factor (EGF) in HeLa cells pretreated with 500-μM vanadate for 30 min; (b) Kinetics of normalized CFP/YFP emission ratios of the Src biosensor in response to 500-μM vanadate in HeLa cells.
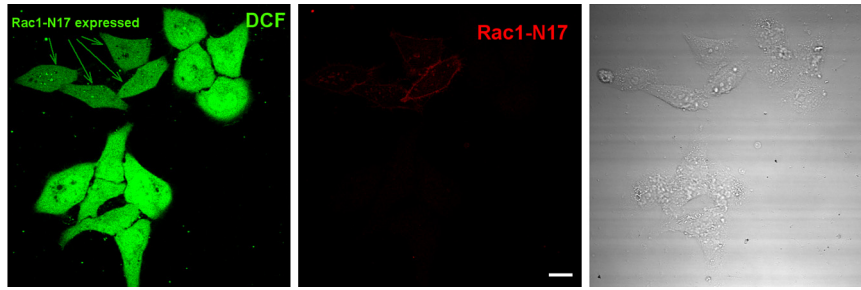
Fig. 3 Carboxy-H$_2$DCFDA, demonstrated Rac1-N17 prevented production of H$_2$O$_2$ in HeLa cells in response to epidermal growth factor (EGF). (Scale bars, 10 μm)
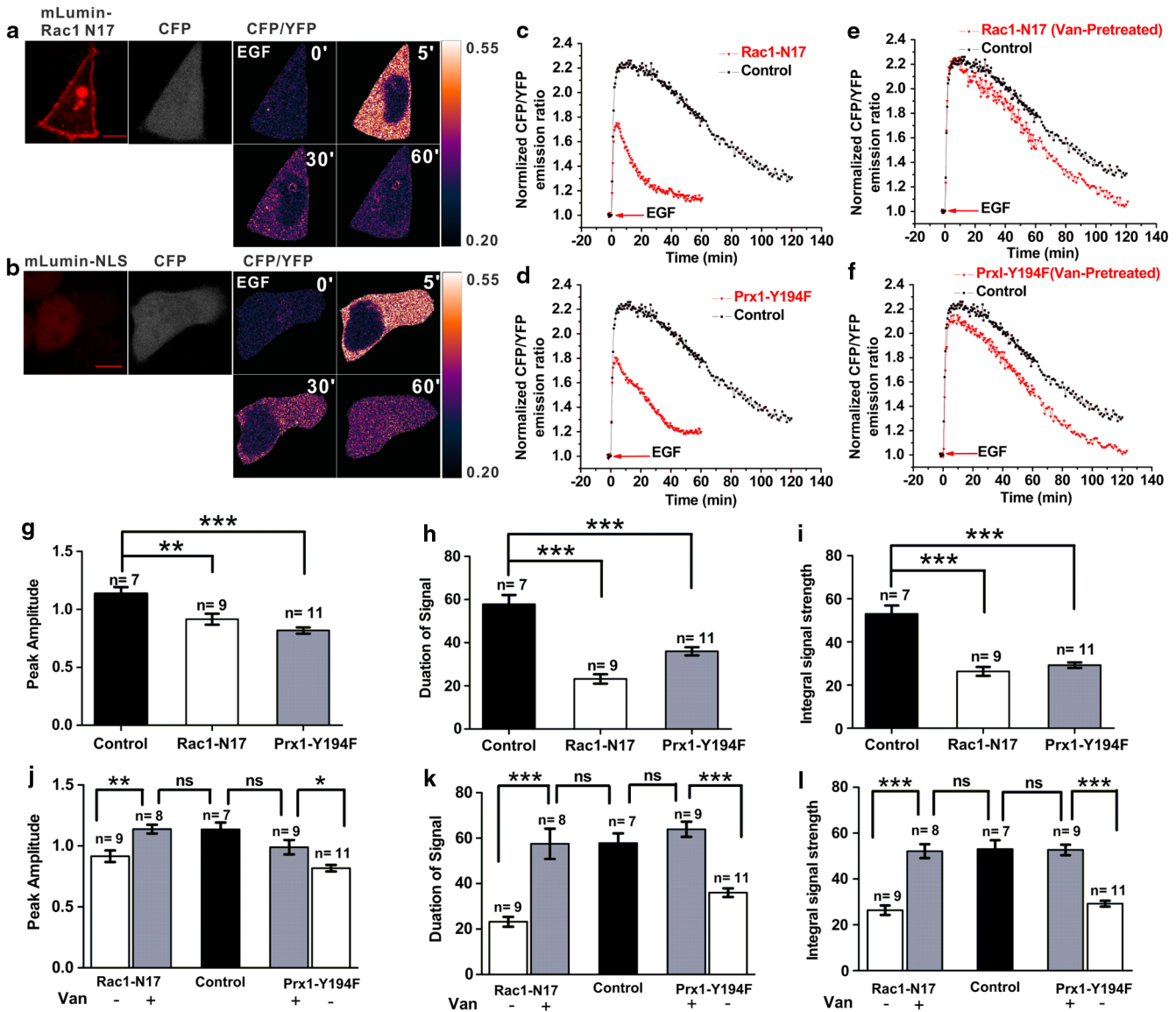

Fig. 4 Overexpression of either mLumin-Rac1-N17 or PrxI-Y194F attenuated epidermal growth factor (EGF)-induced Src signaling in HeLa cells; (a, b) cyan/yellow fluorescent protein (CFP/YFP) emission ratio images of the Src biosensor in a HeLa cell expressing either mLumin-Rac1-N17 or PrxI-Y194F upon EGF treatment. PrxI-Y194F and nuclear-targeted mLumin (mLumin-NLS) were expressed from the same mRNA by using an internal ribosome entry site (IRES) sequences that allowed expression of two genes from the same bi-cistronic mRNA transcript; (c, d) Kinetics of normalized CFP/YFP emission ratios in (a) and (b). (e, f) Kinetics of normalized CFP/YFP emission ratios of the Src biosensor in response to EGF in either Rac1-N17 (e) or PrxI-Y194F-expressing (f) HeLa cells pretreated with 500-μM vanadate (denoted as Van) for 30 min (g, h, i, j, k and l). Bar graphs represent the mean ± standard error (SEM) of peak amplitude (g, j), duration (h, k) and integral signal strength (i, l) of Src signaling from at least three independent experiments with the same conditions as in c, d, e and f. "n" denotes the sample number in each groups. "*", "**" and "***" indicate $p < 0.05$, $p < 0.01$ and, $p < 0.001$, respectively. Scale bars, 10 μm.

enzyme.[37] Previous evidence demonstrated that PrxI is phosphorylated by Src kinase upon EGF stimulation, leading to its inactivation. This inactivation allows localized accumulation of H_2O_2.[38] The PrxI-Y194F protein was demonstrated to be insulated from phosphorylation-mediated inactivation while retaining catalytic activity.[38] Time-lapse imaging of the Src biosensor in PrxI-Y194F-expressing HeLa cells demonstrated that sustained phosphorylation of Src biosensor was attenuated [Fig. 4(b), 4(d), and 4(i); ISS: 29.2 ± 1.3, $n = 11$], strongly implying that H_2O_2 was implicated in maintaining Src signaling. Like in Rac1-N17 transfected cells, the amplitude and duration of Src signaling were both compromised in PrxI-Y194F-expressing HeLa cells [Fig. 4(g) and 4(h)]. PAS was reduced to 0.82 ± 0.03 ($n = 11$; 28% lower than control) and DS was shortened to 36.0 ± 1.9 min ($n = 11$; 38% shorter than control). This result again suggested that H_2O_2 plays a crucial role in maintaining propagation of EGF-induced Src signaling.

Because duration of Src signaling is controlled by PTPs' activity [Fig. 1(d)], we first examined whether the shortened duration of Src signaling resulted from the relatively high PTPs' activity in Rac1-N17 or PrxI-Y194F- expressing cells as compared with the control group. Previous reports demonstrated that growth factor-induced H_2O_2 can inhibit activity of PTPs.[6,7] It is highly likely that overexpressing PrxI-Y194F or Rac1-N17 reduced the amount of H_2O_2 available to inhibit PTPs, leading to the shortened duration of Src signaling. To test this hypothesis, the activity of PTPs in HeLa cells expressing Rac1-N17 or PrxI-Y194F was inhibited with vanadate. The results showed that addition of vanadate increased the duration of the Src signaling in cells expressing either Rac1-N17 [Fig. 4(e) and 4(k); DS: 57.5 ± 6.7 min, $n = 8$] or PrxI-Y194F [Fig. 4(f) and 4(k); DS: 63.9 ± 3.3 min, $n = 9$], verifying our above hypothesis that the activity of PTPs was insufficiently inhibited by H_2O_2 in those cells. Actually, for HeLa cells expressing Rac1-N17 or PrxI-Y194F, vanadate treatment increased the duration of Src signaling to the level of the control group [Fig. 4(k)], indicating that the effect of H_2O_2 on duration of Src signaling is mediated by its inhibition of PTPs. Taken together, we concluded that H_2O_2 modulates the duration of Src signaling through its inhibition of PTPs' activity.

3.3 H_2O_2 Regulates Peak Amplitude of EGF-Induced Src Signaling Through Inhibiting PTP

As indicated in Fig. 4(g), reduction of endogenous H_2O_2 levels by overexpression of Rac1-N17 or PrxI-Y194F led to decreased PAS of Src signaling, suggesting that H_2O_2 is involved in activating Src kinase upon EGF treatment. In cells overexpressing Rac1-N17 or PrxI-Y194F, suppression of PTPs' activity by vanadate not only prolonged the duration of Src signaling, but also increased the peak amplitude of the Src signal [Fig. 4(j); PAS in Rac1-N17-expressed cells: 1.14 ± 0.04, $n = 8$; PAS in PrxI-Y194F-expressed cells: 0.99 ± 0.06, $n = 9$]. Notedly, vanadate treatment recovered the peak amplitude [Fig. 4(j)] of Src signaling in cells expressing Rac1-N17 or PrxI-Y194F to the level of the control group, implying that H_2O_2 enhances Src activation through suppressing PTPs' activity.

To further clarify the role of H_2O_2 on Src activity, we utilized exogenous H_2O_2 to examine its effect on the peak amplitude of EGF-induced Src signaling.[39] Three concentration gradients of H_2O_2 (100-μM, 500-μM, and 1-mM H_2O_2) were used. When compared to the control group, both 500-μM and 1-mM H_2O_2 were able to enhance the PAS of EGF-induced Src signaling

[Fig. 5(a) and 5(b)]. Notably, 100-μM H_2O_2 impaired EGF-induced Src signaling [Fig. 5(a) and 5(b); PAS: 0.60 ± 0.04, $n = 9$]. This phenomenon is explained in the next section.

In the following, we used 1-mM H_2O_2. In HeLa cells expressing Rac1-N17 or Prx1-Y194F, addition of 1-mM H_2O_2 effectively rescued the peak amplitude of EGF-induced Src signaling [Fig. 5(c), 5(d), and 5(e)]. Given that H_2O_2 is a robust inhibitor of PTP,[5,6] and that vanadate could rescue the peak amplitude of Src signaling in cells expressing Rac1-N17 or Prx1-Y194F [Fig. 4(j)], the ability of exogenous H_2O_2 to enhance Src activation could be attributed to its inhibition of PTPs' activity. In fact, it has been reported that Src activity is regulated by H_2O_2-mediated oxidation at cysteine residues.[20] Nevertheless, the consequences (e.g., activation versus inactivation) of H_2O_2-dependent Src oxidation are in conflict.[21–25] Our results suggested that, in the context of an EGF-induced signal transduction pathway, H_2O_2-dependent Src oxidation per se does not exert an essential effect on Src activity. Collectively, we concluded that H_2O_2 regulates the peak amplitude of the EGF-induced Src signaling by inhibiting PTPs' activity.

Notably, the kinetic profile of Src signaling displayed a striking difference in Rac1-N17-expressing HeLa cells upon treatment of EGF and 1-mM H_2O_2 [Fig. 5(d)]. The Src signaling rapidly declined to a low stable level at approximately 30 min, indicating that most Src biosensors were recovered in the dephosphorylation state. Since dephosphorylation of the Src biosensor is specifically mediated by action of PTPs, we reasoned that the rapidly decrease of the CFP/YFP emission ratio (Src signaling) was due to recovery of PTPs' activity after temporary inhibition. To test this hypothesis, we pre-treated HeLa cells with vanadate. As demonstrated by Fig. 5(f), the CFP/YFP emission ratio remained stable during the imaging session, supporting above hypothesis. Thus, we verified again that H_2O_2 tunes the duration of EGF-induced Src signaling through its inhibition of PTPs' activity. The values of three kinetic parameters under different experimental conditions are summarized in Table 1.

3.4 Global Elevation of Intracellular H_2O_2 Level Suppresses Propagation of EGF-Induced Src Signaling

Evidence suggests H_2O_2 is locally produced to specifically organize H_2O_2 signaling events upon growth factor stimulation.[15,40] However, the consequences for growth factor-induced signaling under global elevation of intracellular H_2O_2 level are unclear. In the above section, we determined that low concentration of exogenous H_2O_2 (100-μM) impaired EGF-induced Src signaling [Fig. 5(a) and 5(b)]. We reasoned that exogenous H_2O_2 would cause a global change in cellular redox state, leading to oxidative stress and inevitably triggering cellular antioxidant defenses, which might be implicated in regulating Src signaling. Because the glutathione (GSH) based redox buffer system is the major mechanism for resisting oxidative stress,[41,42] we attempted to determine the kinetics of the GSH-GSSG equilibrium by employing a Grx1-roGFP2 biosensor.[43] The 405/488-nm excitation ratio of Grx1-roGFP2 in cells reflects the ratio of reduced form of glutathione (GSH) and oxidized form of glutathione (GSSG). Under oxidative stress, GSH is converted to GSSG, leading to reduction of GSH-GSSG ratio, which can be reflected by the increase of 405/488-nm excitation ratio of Grx1-roGFP2. As indicated in Fig. 6(a) and 6(b), the GSH-GSSG ratio exhibited a transient decrease
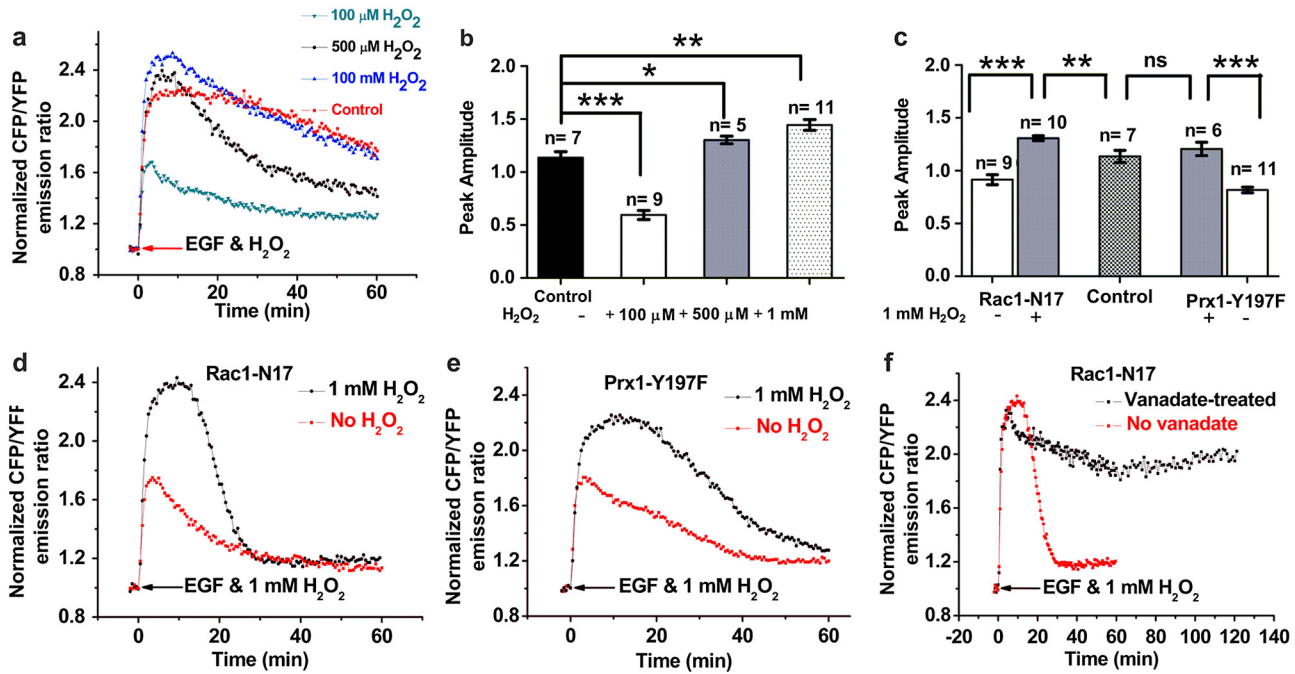
Fig. 5 The impact of exogenous H_2O_2 on the kinetics of epidermal growth factor (EGF)-induced Src signaling in HeLa cells; (a) Kinetics of normalized cyan/yellow fluorescence protein (CFP/YFP) emission ratios of the Src biosensor in HeLa cells in response to EGF and H_2O_2. Three concentration gradients of H_2O_2 (100 μM, 500 μM, and 1 mM H_2O_2) were used. (b) Bar graphs represent the mean $\pm$ standard error (SEM) of peak amplitude of Src signaling in (a). The statistical results were from at least five independent experiments (c). Bar graphs represent the mean $\pm$ SEM of peak amplitude of Src signaling from at least five independent experiments in d and e; (d and e) Kinetics of normalized CFP/YFP emission ratios of the Src biosensor in response to EGF and 1-mM H_2O_2 in either Rac1-N17 (d) or PrxI-Y194F-expressing (e) HeLa cells. (f) Kinetics of normalized CFP/YFP emission ratios of the Src biosensor in response to EGF and 1-mM H_2O_2 in either Rac1-N17- expressing HeLa cells pretreated with 500-μM vanadate for 30 min. "n" denotes the sample number in each group. "*", "**" and "***" indicate $p < 0.05$, $p < 0.01$ and $p < 0.001$, respectively.

and rapid recovery, returning to the basal level within 10 min upon treatment with 100-μM H_2O_2 alone or together with EGF. The GSH-GSSG ratio typically reached a minimum at approximately 2 min. On the contrary, it takes more time for cells to remove higher concentrations of H_2O_2 (500 μM and 1 mM) as indicated in Fig. 6(a) (typically 15–20 min). This finding suggested that cells possess a powerful H_2O_2 elimination system, which might explain the results in Fig. 5(a). Because EGF-induced Src signal typically reach peak within 5 min, we hypothesized that the H_2O_2 degradation system triggered by low exogenous H_2O_2 would also act to remove the endogenous

H_2O_2 that was induced by EGF for inhibition of PTPs' activity. This removal would thus result in impairment of Src signaling. For higher concentration of H_2O_2 (500 μM and 1 mM), the exogenous H_2O_2 would instead enhance the peak amplitude of Src signal because cells are unable to eliminate such high concentration of H_2O_2 within 5 min.

The GSH-GSSG redox buffer system could also explain the distinct Src signaling profile in Fig. 5(d) (EGF and 1-mM H_2O_2). For cells co-expressing Rac1-N17 and Grx1-roGFP2, the 405/488-nm excitation ratio rapidly increased following addition of EGF and 1-mM H_2O_2, and eventually declined to
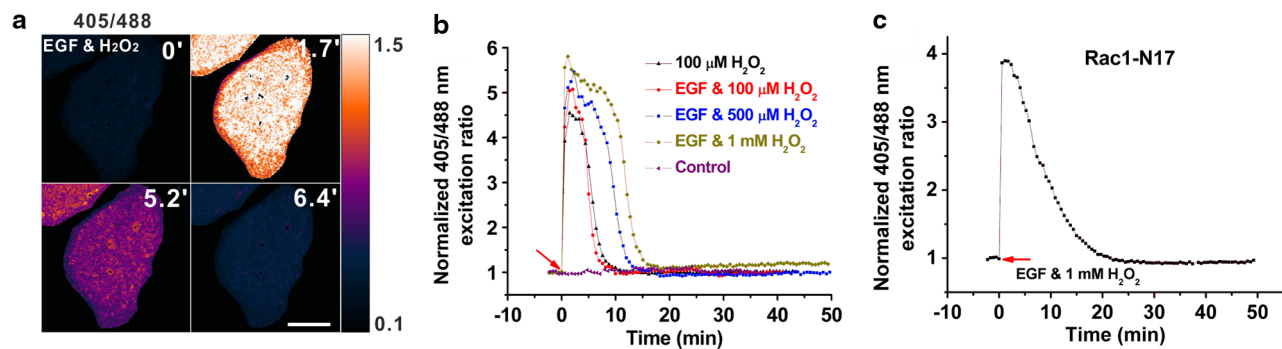

Fig. 6 Imaging of GSH-GSSG ratio kinetics by the Grx1-roGFP2 biosensor in HeLa cells in response to treatment with epidermal growth factor (EGF) and H_2O_2; (a) The 405/488-nm excitation ratio images of Grx1-roGFP2 in a HeLa cell in response to EGF, and (b) time course of normalized 405/488-nm excitation ratios of Grx1-roGFP2 in response to different concentrations of H_2O_2(100 μM, 500 μM, and 1 mM) alone or EGF and 100-μM H_2O_2 as in (a); (c) time course of normalized 405/488-nm excitation ratios of Grx1-roGFP2 in Rac1-N17-expressing HeLa cells in response to EGF and 1-mM H_2O_2. Scale bars, 10 μm.

Table 1 Quantification of EGF-induced Src signaling with three parameters (Mean ± SEM). "N.A" indicates that the data is not given because the groups displayed distinct temporal profiles of EGF-induced Src signaling.

Experimental group	Peak amplitude of Src signal (PAS)	Duration of Src signal (DS)	Integral signal strength (ISS)
Control	1.14 ± 0.06 (n = 7)	57.9 ± 4.2 (n = 7)	53.1 ± 3.8 (n = 7)
500 μM Vanadate	1.33 ± 0.06 (n = 6)	110.8 ± 8.4 (n = 6)	78.7 ± 2.8 (n = 6)
200 nM PP1	0.74 ± 0.05 (n = 8)	56.0 ± 3.3 (n = 8)	35.0 ± 3.4 (n = 8)
100 μM H_2O_2	0.60 ± 0.04 (n = 9)	N.A	N.A
500 μM H_2O_2	1.30 ± 0.04 (n = 5)	N.A	N.A
1 mM H_2O_2	1.44 ± 0.05 (n = 11)	N.A	N.A
Rac1-N17	0.92 ± 0.05 (n = 9)	23.2 ± 2.2 (n = 9)	26.4 ± 2.1 (n = 9)
Rac1-N17 & 500 μM Vanadate	1.14 ± 0.04 (n = 8)	57.5 ± 6.7 (n = 8)	52.1 ± 3.0 (n = 8)
Rac1-N17 & 1 mM H_2O_2	1.31 ± 0.02 (n = 10)	N.A	N.A
Prx1-Y194F	0.82 ± 0.03 (n = 11)	36.0 ± 1.9 (n = 11)	29.2 ± 1.3 (n = 11)
Prx1-Y194F & 500 μM Vanadate	0.99 ± 0.06 (n = 9)	63.9 ± 3.3 (n = 9)	52.7 ± 2.3 (n = 9)
Prx1-Y194F & 1 mM H_2O_2	1.21 ± 0.06 (n = 6)	N.A	N.A

Note: "N.A." = "Not Applicable"

basal levels at approximately 20 min, indicating that the balance of GSH-GSSG was recovered [Fig. 6(c)]. Notably, the recovery of GSH-GSSG balance was a few minutes ahead of the low stable level of Src signaling in Fig. 5(d), strongly suggesting that GSH-dependent removal of H_2O_2 accounts for recovery of PTPs' activity,[44] leading to decreased Src signaling.

In summary, we concluded that global elevation of intracellular H_2O_2 level can attenuate EGF-induced Src signaling. This evidence also suggests that EGF-induced H_2O_2 has to be locally generated. Otherwise, it triggers antioxidant defenses, leading to attenuation of EGF signal transduction.

4 Discussion

Although a substantial body of evidence supports the hypothesis that H_2O_2 signaling plays a vital role in modulating tyrosine phosphorylation signaling, there were no high-quality spatiotemporal dynamic data illustrating the impact of up-regulation or down-regulation of H_2O_2 signaling on the kinetics of tyrosine phosphorylation signaling in living cells. In this study, by dissecting the kinetics of EGF-induced Src signaling with three mathematical parameters that possess specific biological implications, we conclude that H_2O_2 modulates the amplitude and duration of Src signaling by inhibiting PTP activity. Moreover, our results suggest the effect of H_2O_2 on Src activation is mediated by H_2O_2-dependent inhibition of PTPs. And, oxidization of Src might not be essential for activation of Src in EGF-induced signal transduction pathway.

Previous mathematical models concerning protein phosphorylation signaling proposed that signal amplitude was primarily controlled by kinases, whereas phosphatases had more effect on signal duration.[8,9] These principles have been experimentally tested in EGF-induced ERK activation.[8] Our real-time data on the kinetics of EGF-induced Src signaling quantitatively confirms these principles are also true in living cells. The previous

hypothesis about kinetics of tyrosine phosphorylation signaling ignores the crosstalk regulation between kinases (PTKs) and phosphatases (PTPs), and other mechanism (such as H_2O_2) in modulating those two enzymes.[8] In this study, we provided kinetic evidence suggesting that PTPs negatively regulate amplitude of Src signaling by inhibiting Src activation. Furthermore, we also suggested that H_2O_2 is a crucial signaling molecule for modulating the kinetics of EGF-induced Src signaling through its inhibition of PTPs. This mechanism might be extended to other tyrosine phosphorylation signaling cascades, including ERK signal cascades.

The genetically encoded Src biosensor has advantages over cell-based approaches such as immunoblotting or *in vitro* approaches using purified Src in studying the role of H_2O_2 on Src activity. The current data regarding the regulation of Src kinase by H_2O_2 are conflicting. Both activation[21,22] and inactivation[25,45,46] of Src kinase by H_2O_2 have been reported. One reason for such inconsistency might result from varying research approaches. *In vitro* assays exclude the impact of other regulatory mechanisms, such as tyrosine phosphorylation and protein-protein interaction, on the activation of Src.[23,25] Cell-based assays, such as immunoblotting, make use of specific anti-bodies against Tyr416- phosphorylated Src or Tyr 527- phosphorylated Src after cell lysis.[21,45,46] The underlying assumption of these studies is phosphorylation of Tyr416 represents the active state of Src, and phosphorylation of Tyr527 represents the inactive state of Src.[47] However, the cellular consequences of Tyr416 or Tyr527 phosphorylation on the overall activity of Src are elusive. For example, James et al. demonstrated that, for Src familiar member Lck, phosphorylation of Tyr394 at the activation loop of the catalytic domain (corresponding to the Tyr416 residue in Src) is dominant over inhibitory modulation by phosphorylation of Tyr 505 (corresponding to Tyr527 residue in Src).[48] It has also been

demonstrated that PTP members, such as PTP-1B[49] and PTP α,[50] can activate Src kinase by dephosphorylating Tyr527. However, in EGF-induced transduction, nearly 40% of PTP1B is oxidized, suggesting that PTP1B is not likely to activate Src by dephosphorylating Tyr-527.[6] It is possible that Src kinase undergoes activation through distinct mechanisms under different circumstances. Furthermore, the buffer environment of cell lysis, immunoprecipitation and immunoblotting are likely to alter the redox state of Src. Because PTKs and PTPs work in concert to regulate tyrosine phosphorylation, it has been difficult to distinguish the effects of oxidative stress mediated by kinase activation from those caused by phosphatase inhibition. In case of Src, direct regulation of Src itself by phosphatase further deteriorates the accurate clarification of the triangle relationships between Src, H_2O_2 and phosphatases. Therefore, it might be unreliable to directly correlate the effects of Src oxidation with phosphorylation of Tyr418 or Tyr527. In contrast, real-time imaging of the Src biosensor in living cells authentically probes the overall activity of Src, integrating the impact of all factors that are implicated in modulating Src activation. Our results suggest that, *in vivo*, direct oxidization of Src is not essential for its activation in the EGF-induced signal pathway. The effect of H_2O_2 on Src activation is mediated by H_2O_2-dependent inhibition of PTPs [Fig. 4(j)]. Actually, Giannoni et al. demonstrated that the activation of Src in early phases of cell adhesion did not require ROS involvement, although ROS is absolutely necessary to activate Src in later phases of cell adhesion.[21]

In contrast to inconsistencies in the literature concerning the modulation of Src kinase by H_2O_2, the inactivation of phosphatases by H_2O_2 is well established.[5–7] The H_2O_2 is mild oxidant and is not efficient in oxidizing PTPs at the low concentration. For example, for PTP1B (one member of PTPs), the rate constants for H_2O_2 is 9 M^{-1} s^{-1}.[51,52] At a low concentration of 1-μM H_2O_2, the half-time for inactivating PTP1B is about 21 h.[52] This time scale disagrees with the fact that PTP1B participate in rapid signal transduction induced by growth factor.[2,6] Hence, growth factors should induce high concentration of localized H_2O_2 in order to efficiently oxidize PTPs. For instance, PDGF can generate up to 1-mM H_2O_2.[4] At a high concentration of 1-mM H_2O_2, the half-time for inactivating PTP1B is about 1.28 min, agreeing with the fact that *in vivo*, PTPs are rapidly oxidized following administration of EGF.[2,6] Therefore, an EGF-induced, high concentration of localized H_2O_2 can readily oxidize PTPs *in vivo*.[6] Current hypothesis asserts that H_2O_2-mediated PTPs' inhibition is required for strong propagation of ligand-induced tyrosine phosphorylation signaling[5,6,53] because fully active PTPs have substantially higher catalytic activity than tyrosine kinases (up to three orders of magnitude higher than that of tyrosine kinases).[54] This intrinsic mechanism is reflected in the rapidly increase of Src signaling upon EGF stimulation [Fig. 1(b)].

Our results also suggest that EGF-induced H_2O_2 has to be locally produced to bypass cellular antioxidant defenses, which is consistent with the report that EGF does not induce global alteration of the GSH/GSSG redox couple.[40,55] We observed that EGF-induced Src activation was impaired by exogenously adding 100 μM H_2O_2 [Fig. 5(a) and 5(b)], in agreement with the report by Tang et al.[45] However, Tang et al. proposed that the bluntness of EGF-induced Src activation by H_2O_2 is attributed to the inhibition of PTPs' activity. Our current study implies that the activation of H_2O_2-eliminating enzymes

might be the underlying reason for this phenomenon. The fast recovery of the GSH-GSSH balance upon treatment with EGF and 100 μM H_2O_2 suggested that the H_2O_2-degrading enzymes rapidly degrade exogenously H_2O_2 [Fig. 6(b)]. As a result, the endogenous H_2O_2 that is locally and abundantly induced by EGF for activating Src signaling is also inevitably removed, leading to attenuation of Src signaling [Fig. 5(a) and 5(b)]. Instead, higher concentration of exogenous H_2O_2 are able enhance Src signal because cells are incapable of removing such levels of exogenous H_2O_2 within short period. Glutathione peroxidase 1 (GPx1) may be a potential candidate for a H_2O_2 removing enzyme.[56] Gpx1 has been reported to be activated by c-Abl via phosphorylation,[57] and c-Abl itself can be activated by oxidative stress.[58] Additional work needs to be done to test this hypothesis.

In summary, we have obtained substantial evidence concerning the crucial role of H_2O_2 in regulating kinetics of EGF-induced Src signaling in living cells, which offers new insight into kinetic mechanism of tyrosine phosphorylation signaling *in vivo*. Additionally, our research approach, which analyzes the FRET-biosensor derived kinetic data with mathematical parameters, is inspirational to elucidation of spatiotemporal regulatory mechanisms of different signal pathways in living cells.

Acknowledgments

Appendix: Procedures

Measurement of intracellular hydrogen peroxide production by confocal microscopy: Intracellular production of H_2O_2 was assayed after treatment of cells with EGF (100 ng/ml) in serum-free Dulbecco's modified Eagle's medium. After incubation for 10 min, cells were washed with HBSS (Hanks' balanced salt solution) and incubated for 15 min in the dark at 37°C with HBSS loading buffer containing 2-μM carboxy-H_2DCFDA. Non-fluorescent carboxy-H_2DCFDA is oxidized by H_2O_2 to highly fluorescent DCF and retained by cell. Then, loading buffer was removed and cells were returned to pre-warm the serum-free DMEM. Cells were then examined using the FV1000 confocal laser scanning microscope (Olympus, Japan) with excitation at 488 nm and fluorescence acquired from 500 to 540 nm.

References

1. S. G. Julien et al., "Inside the human cancer tyrosine phosphatome," *Nat. Rev. Cancer* **11**(1), 35–49 (2011).

2. Y. S. Bae et al., "Epidermal growth factor (EGF)-induced generation of hydrogen peroxide—role in EGF receptor-mediated tyrosine phosphorylation," *J. Bio. Chem.* **272**(1), 217–221 (1997).

3. J. C. Juarez et al., "Superoxide dismutase 1 (SOD1) is essential for H2O2-mediated oxidation and inactivation of phosphatases in growth factor signaling," *P. Natl. Acad. Sci. USA* **105**(20), 7147–7152 (2008).

4. M. Sundaresan et al., "Requirement for generation of H_2O_2 for platelet-derived growth factor signal transduction," *Science* **270**(5234), 296–299 (1995).

5. P. Chiarugi and F. Buricchi, "Protein tyrosine phosphorylation and reversible oxidation: two cross-talking posttranslation modifications," *Antioxid. Redox. Sign.* **9**(1), 1–24 (2007).

6. S. R. Lee et al., "Reversible inactivation of protein-tyrosine phosphatase 1B in A431 cells stimulated with epidermal growth factor," *J. Bio. Chem.* **273**(25), 15366–15372 (1998).

7. P. Chiarugi et al., "Two vicinal cysteines confer a peculiar redox regulation to low molecular weight protein tyrosine phosphatase in response to platelet-derived growth factor receptor stimulation," *J. Bio. Chem.* **276**(36), 33478–33487 (2001).

8. J. J. Hornberg et al., "Principles behind the multifarious control of signal transduction—ERK phosphorylation and kinase/phosphatase control," *Febs. J.* **272**(1), 244–258 (2005).

9. R. Heinrich, B. G. Neel, and T. A. Rapoport, "Mathematical models of protein kinase signal transduction," *Mol. Cell* **9**(5), 957–970 (2002).

10. M. Ebisuya, K. Kondoh, and E. Nishida, "The duration, magnitude and compartmentalization of ERK MAP kinase activity: mechanisms for providing signaling specificity," *J. Cell. Sci.* **118**(14), 2997–3002 (2005).

11. C. J. Marshall, "Specificity of receptor tyrosine kinase signaling: transient versus sustained extracellular signal-regulated kinase activation," *Cell* **80**(2), 179–185 (1995).

12. Y. X. Wang, J. Y. J. Shyy, and S. Chien, "Fluorescence proteins, live-cell imaging, and mechanobiology: seeing is believing," *Annu. Rev. Biomed. Eng.* **10**, 1–38(2008).

13. J. Zhang et al., "Creating new fluorescent probes for cell biology," *Nat. Rev. Mol. Cell. Bio.* **3**(12), 906–918 (2002).

14. A. Ibraheem and R. E. Campbell, "Designs and applications of fluorescent protein-based biosensors," *Curr. Opin. Chem. Bio.* **14**(1), 30–36 (2010).

15. N. M. Mishina et al., "Does cellular hydrogen peroxide diffuse or act locally?," *Antioxid. Redox. Sign.* **14**(1), 1–7 (2011).

16. D. Wang et al., "Genetically encoded ratiometric biosensors to measure intracellular exchangeable zinc in Escherichia coli," *J. Biomed. Opt.* **16**(8), 087011 (2011).

17. T. Bruns et al., "Forster resonance energy transfer-based total internal reflection fluorescence reader for apoptosis," *J. Biomed. Opt.* **14**(2), 021003 (2009).

18. G. S. Martin, "The road to Src," *Oncogene.* **23**(48), 7910–7917 (2004).

19. T. J. Yeatman, "A renaissance for SRC," *Nat. Rev. Cancer* **4**(6), 470–480 (2004).

20. E. Giannoni, M. L. Taddei, and P. Chiarugi, "Src redox regulation: again in the front line," *Free Radical Bio. Med.* **49**(4), 516–527 (2010).

21. E. Giannoni et al., "Intracellular reactive oxygen species activate Src tyrosine kinase during cell adhesion and anchorage-dependent cell growth," *Mol. Cell. Bio.* **25**(15), 6391–6403 (2005).

22. J. Abe et al., "c-Src is required for oxidative stress-mediated activation of big mitogen-activated protein kinase 1 (BMK1)," *J. Bio. Chem.* **272**(33), 20389–20394 (1997).

23. E. K. Krasnowska et al., "N-acetyl-l-cysteine fosters inactivation and transfer to endolysosomes of c-Src," *Free Radical Bio. Med.* **45**(11), 1566–1572 (2008).

24. H. Tang et al., "Inactivation of Src family tyrosine kinases by reactive oxygen species in vivo," *J. Biol. Chem.* **280**(25), 23918–23925 (2005).

25. D. J. Kemble and G. Q. Sun, "Direct and specific inactivation of protein tyrosine kinases in the Src and FGFR families by reversible cysteine oxidation," *Proc. Natl. Acad. Sci. USA* **106**(13), 5070–5075 (2009).

26. Y. X. Wang et al., "Visualizing the mechanical activation of Src," *Nature* **434**(7036), 1040–1045 (2005).

27. M. X. Ouyang et al., "Determination of hierarchical relationship of Src and Rac at subcellular locations with FRET biosensors," *P. Natl. Acad. Sci. USA* **105**(38), 14353–14358 (2008).

28. G. Huyer et al., "Mechanism of inhibition of protein-tyrosine phosphatases by vanadate and pervanadate," *J. Bio. Chem.* **272**(2), 843–851 (1997).

29. J. Chu et al., "A novel far-red bimolecular fluorescence complementation system that allows for efficient visualization of protein interactions under physiological conditions," *Biosens. Bioelectron.* **25**(1), 234–239 (2009).

30. J. Brons-Poulsen et al., "An improved PCR-based method for site directed mutagenesis using megaprimers," *Mol. Cell. Probe.* **12**(6), 345–348 (1998).

31. Y. C. Poh et al., "Rapid activation of rac GTPase in living cells by force is independent of Src," *Plos. One.* **4**(11), e7886–e7886 (2009).

32. O. Pertz et al., "Spatiotemporal dynamics of RhoA activity in migrating cells," *Nature* **440**(7087), 1069–1072 (2006).

33. R. H. Cool et al., "Rac1, and not Rac2, is involved in the regulation of the intracellular hydrogen peroxide level in HepG2 cells," *Biochem. J.* **332**(Pt 1), 5–8 (1998).

34. Y. S. Bae et al., "Platelet-derived growth factor-induced H_2O_2 production requires the activation of phosphatidylinositol 3-kinase," *J. Bio. Chem.* **275**(14), 10527–10531 (2000).

35. H. S. Park et al., "Sequential activation of phosphatidylinositol 3-kinase, beta Pix, Rac1, and Nox1 in growth factor-induced production of H_2O_2," *Mol. Cell Bio.* **24**(10), 4384–4394 (2004).

36. T. L. Leto et al., "Targeting and regulation of reactive oxygen species generation by nox family NADPH oxidases," *Antioxid. Redox. Sign.* **11**(10), 2607–2619 (2009).

37. S. G. Rhee, H. Z. Chae, and K. Kim, "Peroxiredoxins: a historical overview and speculative preview of novel mechanisms and emerging concepts in cell signaling," *Free Radical Bio. Med.* **38**(12), 1543–1552 (2005).

38. H. A. Woo et al., "Inactivation of peroxiredoxin I by phosphorylation allows localized H_2O_2 accumulation for cell signaling," *Cell* **140**(4), 517–528 (2010).

39. H. J. Forman, "Use and abuse of exogenous H_2O_2 in studies of signal transduction," *Free Radical Bio. Med.* **42**(7), 926–932 (2007).

40. S. Cuddihy, C. C. Winterbourn, and M. B. Hampton, "Assessment of redox changes to hydrogen peroxide-sensitive proteins during EGF signaling," *Antioxid. Redox. Sign.* **15**(1), 167–174 (2011).

41. S. G. Rhee et al., "Controlled elimination of intracellular H_2O_2: regulation of peroxiredoxin, catalase, and glutathione peroxidase via posttranslational modification," *Antioxid. Redox. Sign.* **7**(5–6), 619–626 (2005).

42. C. F. Ng et al., "The rate of cellular hydrogen peroxide removal shows dependency on GSH: mathematical insight into in vivo H_2O_2 and GPx concentrations," *Free Radical Res.* **41**(11), 1201–1211 (2007).

43. M. Gutscher et al., "Real-time imaging of the intracellular glutathione redox potential," *Nat. Meth.* **5**(6), 553–559 (2008).

44. W. C. Barrett et al., "Roles of superoxide radical anion in signal transduction mediated by reversible regulation of protein-tyrosine phosphatase 1B," *J. Bio. Chem.* **274**(49), 34543–34546 (1999).

45. H. Tang et al., "Inactivation of Src family tyrosine kinases by reactive oxygen species in vivo," *J. Bio. Chem.* **280**(25), 23918–23925 (2005).

46. J. M. Cunnick et al., "Role of tyrosine kinase activity of epidermal growth factor receptor in the lysophosphatidic acid-stimulated mitogen-activated protein kinase pathway," *J. Bio. Chem.* **273**(23), 14468–14475 (1998).

47. G. Q. Sun et al., "Effect of autophosphorylation on the catalytic and regulatory properties of protein tyrosine kinase Src," *Arch. Biochem. Biophys.* **397**(1), 11–17 (2002).

48. J. S. Hardwick and B. M. Sefton, "The activated form of the Lck tyrosine protein kinase in cells exposed to hydrogen peroxide is phosphorylated at both Tyr-394 and Tyr-505," *J. Bio. Chem.* **272**(41), 25429–25432 (1997).

49. J. D. Bjorge, A. Pang, and D. J. Fujita, "Identification of protein-tyrosine phosphatase 1B as the major tyrosine phosphatase activity capable of dephosphorylating and activating c-Src in several human breast cancer cell lines," *J. Bio. Chem.* **275**(52), 41439–41446 (2000).

50. X. M. Zheng, R. J. Resnick, and D. Shalloway, "A phosphotyrosine displacement mechanism for activation of Src by PTP alpha," *Embo. J.* **19**(5), 964–978 (2000).

51. J. R. Stone, "An assessment of proposed mechanisms for sensing hydrogen peroxide in mammalian systems," *Arch. Biochem. Biophys.* **422**(2), 119–124 (2004).

52. J. N. LaButti et al., "Redox regulation of protein tyrosine phosphatase 1B by peroxymonophosphate ($-O3POOH$)," *J. Am. Chem. Soc.* **129**(17), 5320–5321 (2007).

53. H. E. Grecco, M. Schmick, and P. I. H. Bastiaens, "Signaling from the living plasma membrane," *Cell* **144**(6), 897–909 (2011).

54. E. H. Fischer, H. Charbonneau, and N. K. Tonks, "Protein tyrosine phosphatases: a diverse family of intracellular and transmembrane enzymes," *Science* **253**(5018), 401–406 (1991).

55. P. J. Halvey et al., "Compartmental oxidation of thiol-disulphide redox couples during epidermal growth factor signalling," *Biochem. J.* **386**(Pt 2), 215–219 (2005).

56. R. Brigelius-Flohe and A. Kipp, "Glutathione peroxidases in different stages of carcinogenesis," *Bba-Gen. Subjects* **1790**(11), 1555–1568 (2009).

57. C. Cao et al., "Glutathione peroxidase 1 is regulated by the c-Abl and Arg tyrosine kinases," *J. Bio. Chem.* **278**(41), 39609–39614 (2003).

58. X. G. Sun et al., "Activation of the cytoplasmic c-Abl tyrosine kinase by reactive oxygen species," *J. Bio. Chem.* **275**(23), 17237–17240 (2000).